Available online at www.sciencedirect.com
SCIENCE DIRECT®
Thin Solid Films 498 (2006) 183 – 187
thin solid films
www.elsevier.com/locate/tsf

Optical recombination-emission characteristics and surface morphologies of InAs quantum dots grown on misoriented GaAs substrate by MOCVD

M.-Y. Hsu [a], S.-F. Tang [b,*], C.-D. Chiang [b], C.-C. Su [a], L.-C. Wang [c], C.-T. Kuo [c]

[a] *National Taipei University of Technology, Taipei 106, Taiwan*
[b] *Chung Shan Institute of Science and Technology, Taoyuan 325, Taiwan*
[c] *National Chiao Tung University, Hsinchu 300, Taiwan*

Available online 22 August 2005

Abstract

The InAs quantum dot (QD) structures grown on (100) 2°, 6°, 10°, 15° off-angles to (111)A GaAs substrate have been investigated by atomic force microscopy (AFM) and cryogenic photoluminescence (PL). The exact-angle InAs/GaAs is used as the reference sample. The blue shift of PL peak spectra with increasing misoriented scales has also been observed experimentally. In this work, we demonstrated that different off-angle substrates would influence the distribution and uniformity of QD due to variant surface potential energies, which are responsible for the two-stage process (migration and nucleation) of InAs adatoms on the off-angle substrates.

Keywords: Metal-organic chemical vapour deposition (MOCVD); PL; AFM; Quantum dot infrared photodetector (QDIP)

1. Introduction

The formation of self-organized arrays of InAs quantum dot on GaAs substrates has attracted much interest due to their applications for nanoscale devices such as quantum dot photodetector, laser diode and other optoelectronic modules [1–3]. It was proposed that modulation of the emission spectra of quantum dots can be obtained by adjusting directly the morphologies of InAs quantum dot arrays [4]. The formation of QD based on the self-organized effect in III–V semiconductor compounds grown by metal-organic chemical vapour deposition (MOCVD) and its varieties have been investigated experimentally in recent years [6–10]. These influences of growth mechanism and conditions on the height, lateral size, surface densities and uniformities of quantum dot arrays using the AFM and PL measurement have been established [5–7]. Most of these factors are controlled by growth kinetics of adatoms and physical setting conditions of growth facility. For instance, the use of step-interruption, submonolayer migration-stimulated epitaxy, and vicinal GaAs substrates is attributed to arrays of InAs QDs grown on the closest lateral step regions and results in the varieties of the PL spectra [10]. The transient nature of various morphologies of AFM and the observations of transitions of PL spectra under cryogenic temperatures from two-dimensional (2D) InAs lateral islands to three-dimensional (3D) InAs dots on larger misoriented GaAs substrate are the main subjects on this paper. The profiles of the PL spectra strongly depend on the distributions of QD arrays, which are responsible for mono-atomic step bunching on terraces having discrete width of vicinal GaAs substrate. The two-stage model of adatom (migration and nucleation) is proposed to explain the growth behaviour of the InAs quantum dot arrays grown on off-angle substrates.

2. Experimental details

All samples used in this paper were grown on off-angle (100) GaAs substrates by metal-organic chemical vapour

* Corresponding author. Tel.: +886 3 4712201x357106; fax: +886 3 4711024.
E-mail address: shiangfengtang@yahoo.com.tw (S.-F. Tang).

0040-6090/$ - see front matter © 2005 Elsevier B.V. All rights reserved.
doi:10.1016/j.tsf.2005.07.078

deposition. An undoped 0.5-μm-thick GaAs buffer layer was deposited under the growth temperature of 585 °C. Subsequently, decreasing the growth temperature to 500 °C and under the V–III beam equivalent pressure ratio of 1–1.8, the 280 sccm TMIn (trimethyl-indium) is kept for injection of the growth chamber for 5 s. The QD arrays on (100) GaAs substrate were prepared with TMIn (trimethyl-indium) and AsH_3 (arsine) as the source material gases. Then AsH_3 is interrupted and retained for 7 s for adatom migration well. The InAs quantum dot arrays were generated under the condition. A 20-nm-thick GaAs spacer layer was grown at the same temperature. The deposited sequence was repeated three times, except for undoped GaAs buffer layer. Finally, the InAs QDs were grown again for AFM measurement. The origin and evolution of the multiple layers based on QD structures of PL spectra were studied in relation to the exact-axis (100) GaAs and 2°, 6°, 10°, 15° off-angles to (111)A (i.e., gallium-rich GaAs facet) of the substrates to verify their effects on structure and morphology of the QD arrays. The different off-angle designations and features of the QD arrays of the specimen are shown in Table 1. In this work, the samples were grown by a metal-organic chemical vapour deposition and put into the growth chamber at the same deposited procedure. The micro-effusion tubes of hydride carrier and reaction gases are distributed uniformly on top gas-plate in growth chamber of MOCVD to improve the deposited uniformity of InAs QD films.

To investigate the surface morphologies of the InAs QDs deposited on different off-angle GaAs substrates, we used Digital Instrument-3100 atomic force microscopy with the taping Si tip. In the photoluminescence measurement, the excited YAG laser with the peak wavelength 532.8 nm is adopted as pumping laser. The maximum incidence power density is 4.97 W/cm^2. The luminescence light from the samples on the CTI-cryogenic chamber was focused into the 2-mm-wide slit on 500-mm-long monochromator, and detected by low-noise Germanium photodetector. The wavelength scanning range, speed and step resolution are from 800 to 1550 nm, 250 nm/min and 2 nm, respectively. The signal was modulated and amplified by the lock-in electronic module, and the time constant is set to 100 ms. The schematics of PL measurement system is shown in Fig. 1 [11]. Besides, we used the optical attenuator to change excited laser power in order to know its influence on these QD samples.

Table 1
The QD structural features on different (100) off-angles to (111)A GaAs substrate

Sample	Off-angles (°)	Dot density ($\times 10^{10}$ cm^{-2})	Lateral diameter (nm)	Height (nm)
a	0	N/A	N/A	N/A
b	2	0.45	8–25	2.5–15
c	6	0.63	20–50	4–12
d	10	4.5	5–30	3–10
e	15	0.35	~20	~4 and ~7.5

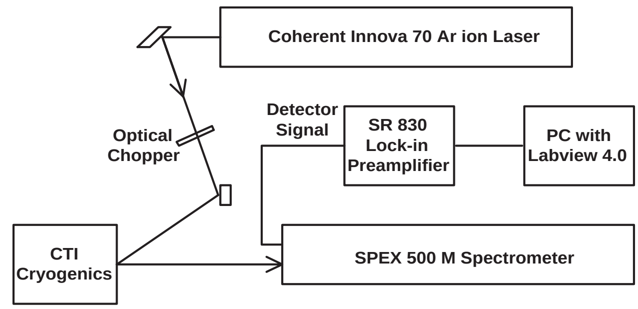

Fig. 1. The schematic of cryogenic PL measurements with optoelectronic accessory.

3. Results and discussions

These 1 μm × 1 μm sized AFM 3D images of InAs QD grown on (100)-oriented GaAs substrate 0°, 2°, 6°, 10°, 15° off-angles to (111)A are shown in Fig. 2(a)–(f). The structural features are summarized in Table 1 (excluded exact-axis InAs/GaAs sample). The QD arrays on reference sample with exact-angle are distributed by the isotropic orientation. The average density and height on InAs dot arrays are 2×10^{10} cm^{-2} and 7.5 nm, respectively, in Fig. 2(a). From Table 1, in sample with 2°off-angle, the dot density decreases abruptly to 4.57×10^{9} cm^{-2} and the localized 2D dots with line-shaped islands are nucleated along the [$\bar{1}$10]-orientation. The larger InAs islands appear in the localized regions near the terraces of GaAs. Compared to the line-shaped islands, the height of 2D InAs dots is much larger as shown in Fig. 2(b). The results obtained propose that the migration rate of indium adatoms on the off-angle substrate is larger than the self-nucleation rate of that along the [$\bar{1}$10]-orientation, which leads to generation of line-shaped and 3D islands for decreasing the total surface bonding energies. The similar observation has happened in the 6° off-angle GaAs substrate. However, it is surprisingly found that no long line-shaped bunching and larger 3D islands appear on the 10° off-angle substrate. The lateral size distribution is highly assembled, i.e., ~20 nm × 20 nm and dot density yield is high. The average density and height on InAs dot arrays are 4×10^{10} cm^{-2} and ~6 nm, respectively. The transient behaviour is explained reasonably by the following elucidation: Though InAs adatoms grown on extreme off-angle GaAs substrate have smaller step width (~25 nm), the surface bonding energies on step edges are larger than those on the flattening ones among the terraces. Thus the contour densities of higher surface bonding energies on 10° off-angle sample become higher compared to that mentioned above. The result leads to the adatom seeding around step edge for decreasing the total surface energies. From the microscopic view, the nucleation process would be continued once the seeding

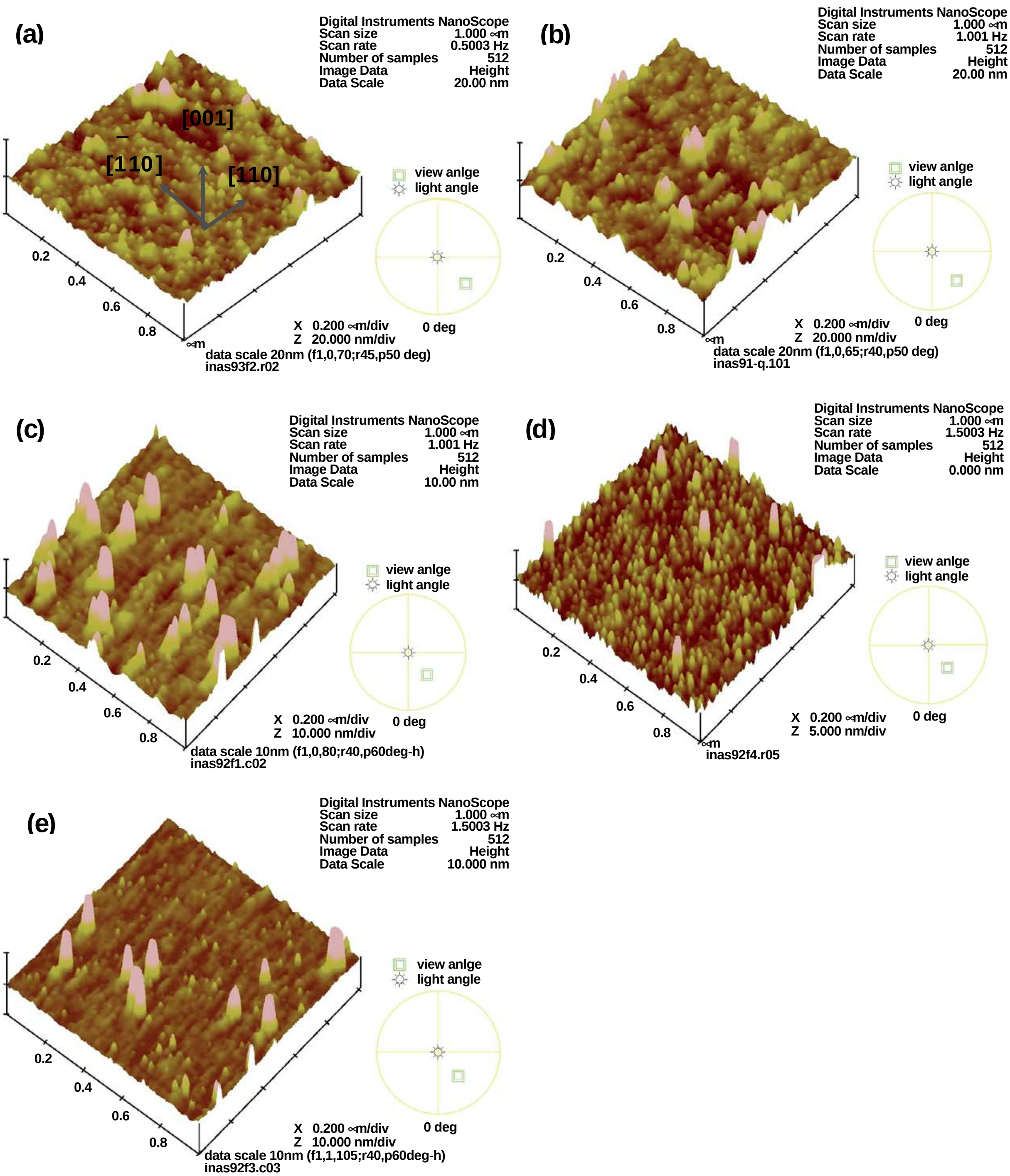

Fig. 2. 3D AFM images of QDs on (100)-oriented GaAs substrate with (a) 0°, (b) 2°, (c) 6°, (d) 10° and (e) 15° off-angles to (111)A, respectively.

generation under background AsH_3 flux (i.e., closed AsH_3 shutter) and extremely low V/III pressure ratio in the growth chamber were achieved. In turn, under the high temperature reaction of TMIn, the indium adatoms deposited on GaAs atomic layer would be re-segregated and then desorbed again from the surface [12,13]. Therefore, the demonstration of the macroscopic observations, due to high contour density of surface energies, is attributed to high dot density. At the same time, the migration rate is much smaller than nucleation rate of the indium adatoms along the $[\bar{1}10]$-orientation. The decreasing surface energies on 10° off-angle substrate are responsible for the behind factor (i.e., nucleation rate). When the QDs are grown on 15° off-angle substrate, the dot density is decreased (about 3.5×10^9 cm^{-2}) and the line-shaped islands on this sample increase. On the other side, the growth mechanism is similar with the 10° off-angle sample. But the GaAs atomic layer spacing is smaller than 20 nm, which limits the lateral size of QDs

[13]. At the same time, the migration rate of the indium adatoms along the [$\bar{1}$10]-orientation is higher than in other directions, thus generating InAs stacked islands easily in this direction. The smaller dot size and line-shaped 2D-islands on 15° off-angle substrate have been exhibited in Fig. 2(e). The extreme variance from 10° to 15° off-angle substrates might be explained by the fact that there is a lower surface GaAs atomic density on 15° off-angle substrate compared to the 10° off-angle, which leads to lower surface binding energies. Thus, the distribution of InAs adatoms has a trend for generating lower 2D islands and smaller QDs.

From the above results, it is quite obvious that the different off-angle substrates have dominant influence on the distribution and uniformity of QD due to variant surface potential energies which are responsible for the two-stage process (migration and nucleation) of InAs adatoms on the off-angle substrates. This model was applied to the cases of quasi-2D islands and 3D dots, which allowed us to explain the features of PL spectra from the InAs quantum dots and islands.

When these exact- and off-angle samples were put into the cryogenic system with auto-feedback temperature controlling, the normalized PL spectra under the temperature of 20 K and the excited power of 4.97 W/cm^2 are exhibited in Fig. 3. The non-radiation process from the thermal influence of these samples would be suppressed efficiently under the extremely low temperature. The concept of a random occupation by carriers of localized QD energy states at low temperature is noted. The QD spectra are commonly deconvoluted into Gaussian components under the assumption that the emission line contour describes the statistical size distribution of QDs [14]. In this case, the recombination emissions of PL spectra come from larger size dominant dots and larger 2D islands. Compared to exact sample, the intensity of peak energy in 2° off-angle sample is much higher in the energy of 1.12 eV and compatible in that of 1.06 eV. It can be concluded that the 2D streaked islands appear, which agreed with the

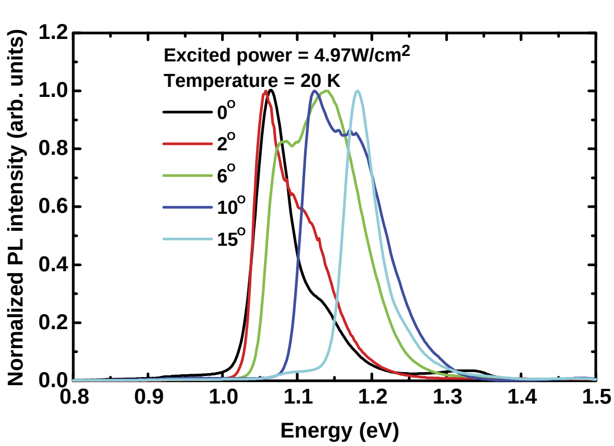

Fig. 3. The PL spectra under temperature of 20 K from 0° to 15° off-angle samples.

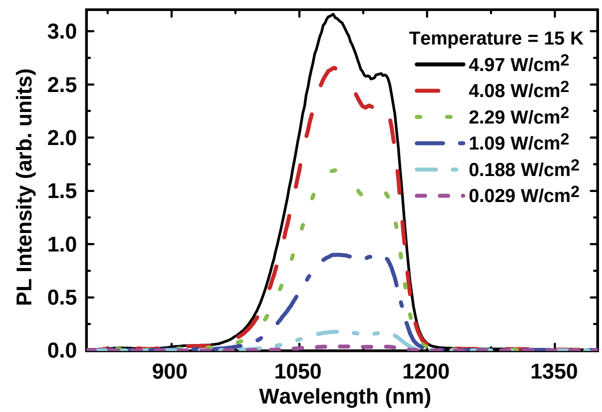

Fig. 4. The PL spectra of QD on (100)-oriented GaAs substrate tilted 6° off-angle to (111)A as a function of excited power density.

AFM data. The FWHM of above samples are similar in Gaussian fitting 1.12 eV due to the assembled QD uniformity, but there is a different dominant dot density in these samples. In the 6° off-angle sample, the higher and lower intensities of peak energies in 1.14 eV and 1.08 eV attribute for smaller dots and larger streaked islands along the [$\bar{1}$10]-orientation. From the 10° off-angle sample in Fig. 3, the two Gaussian fitting curves that are displayed in the peak energies of 1.13 and 1.18 eV relate to two different groups of assembled dots, respectively. The emission spectrum transits from the smallest dominant dots in the extreme 15° off-angle sample. The peak position is from 1.06 eV to 1.18 eV under increasing off-angles. This indicates that the large blue shifts of 120 meV on peak position of energies attribute to the morphologies of InAs adatomic layers when enlarging off-angles. The experimental results of PL spectra under the cryogenic condition follow the AFM measurements. Fig. 4 shows the power-dependent PL spectra of the QD on (100)-oriented GaAs substrate tilted 6° off-angle to (111)A at the temperature of 15 K. It is clear to believe that the band state filling effect happens on larger laser power density beyond 1.09 W/cm^2. Besides, demonstrating the PL spectra at 300 K illustrated in Fig. 5, it is found that the peak wavelength could be pushed to nearly 1.28

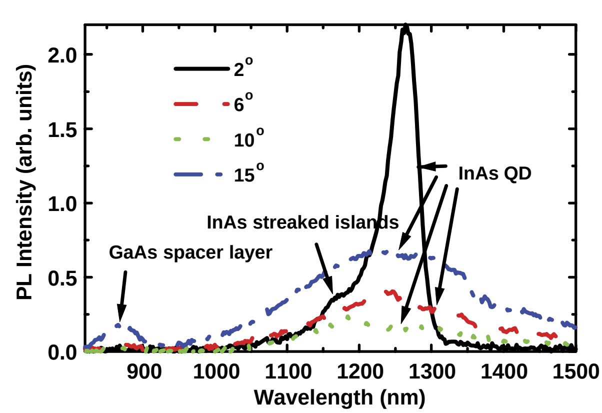

Fig. 5. The PL spectra of QD on off-angle GaAs substrates at room temperature.

μm, and the sample with 2° off-angle substrate has the best optical characteristics at room temperature compared to the other samples. It could attribute to the lowest density of lattice defects on the 2° off-angle substrates. The phenomenon is not clear completely.

4. Conclusions

We have developed a MOCVD technology to grow InAs dots on the off-angle substrates. Different morphological QDs on GaAs and power-excited dependent PL spectra under cryogenic temperature have been demonstrated. Although the assembled dot size density and uniformity of 10° off-angle substrate show the best result from the 3D AFM image, the optical characteristics are dominated by the other epitaxial issue such as lattice defect density on off-angle substrate at room temperature. By using these experimental results, we would well design the high-performance and long-wavelength emission of the opto-electronic devices in the future.

Acknowledgements

The authors thank Dr. W. Lin, Land Mark Optoelectronics Corporation, for participation in the growth experiment, and Dr. S.-Y. Lin for helpful participation in the technological discussions. This work was fully supported by the National Research Program for Nanoscience and Technology.

References

[1] Q. Xie, A. Kalburge, P. Chen, A. Madhukar, IEEE Photonics Technol. Lett. 8 (1996) 965.
[2] P. Bhattacharya, S. Krishna, J. Phillips, P.J. McCann, K. Namjou, J. Cryst. Growth 227/228 (2001) 27.
[3] H. Petterson, L. Baath, N. Carlsson, W. Seifert, L. Samuelson, Appl. Phys. Lett. 79 (2001) 78.
[4] Y. Nabetani, A. Wakahara, A. Sasaki, J. Appl. Phys. 78 (1995) 6461.
[5] Tao Yang, Jun Tatebayashi, Shiro Tsukamoto, Masao Nishioka, Yasuhiko Arakawa, Appl. Phys. Lett. 84 (2004) 2817.
[6] N. Nuntawong, S. Birudavolu, C.P. Hains, S. Huang, H. Xu, D.L. Huffaker, Appl. Phys. Lett. 85 (2004) 3050.
[7] Tao Yang, Shiro Tsukamoto, Jun Tatebayashi, Masao Nishioka, Yasuhiko Arakawa, Appl. Phys. Lett. 85 (2004) 2753.
[8] J. Toušková, E. Samochin, J. Toušek, J. Oswald, E. Hulicius, J. Pangrác, K. Melichar, T. Šimeček, J. Appl. Phys. 91 (2002) 10103.
[9] Theodore Chung, Gabriel Walter, Nick Holonyak Jr., J. Appl. Phys. 97 (2005) 053510.
[10] N. Ikoma, S. Ohkouchi, Jpn. J. Appl. Phys. 34 (1995) L724.
[11] S.F. Tang, S.Y. Lin, S.T. Yang, C.D. Chiang, Y.T. Cherng, H.T. Shen, T.E. Nee, R.M. Lin, M.Y. Hsu, IEEE Trans. Nanotech. 3 (2004) 275.
[12] O. Brandt, L. Tapfer, K. Ploog, Phys. Rev., B, Condens. Matter 44 (1991) 8043.
[13] O. Brandt, G.C. La Rocca, A. Heberle, Phys. Rev., B, Condens. Matter 45 (1992) 3803.
[14] M. Grundmann, R. Heitz, N. Ledentsov, Superlattices Microstruct. 19 (1996) 81.